EURASIP Journal on Advances in Signal Processing

RESEARCH Open Access

Optimization of ACF-DSR-based joint Doppler shift and SNR estimator for Internet of Vehicle system

Jiangang Wen[1], Lei Yan[1], Xiaofei Feng[2], Zhengwei Ni[1], Jingyu Hua[1,3*] and Zhijiang Xu[3]

*Correspondence: eehjy@163.com
[1] School of Information and Electronic Engineering, Zhejiang Gongshang University, Hangzhou 310018, China
Full list of author information is available at the end of the article

Abstract

Accurate vehicle speed estimation is required for intelligent internet of vehicles, and it can be realized by Doppler shift estimation in mobile communication. In this paper, the ACF-DSR (autocorrelation function-double sampling rate) method for joint Doppler shift and SNR estimation is further investigated. Based on the analysis of ACF, an improved algorithm model taking account of estimation deviation is formulated. Then, the effects of sampling intervals in DSR are figured out by mean square error analysis of estimation, and two better choices are obtained. By Monte Carlo simulations, it is demonstrated that the optimized ACF-DSR method with better choice of sampling intervals can achieve better estimation and outperform previous methods.

Keywords: Autocorrelation function, Double sampling rate, Doppler shift, SNR, IoV

1 Introduction

The Internet of Things (IoT) is recognized as one of the most important areas of future technology and is gaining vast attention from a wide range of industries [1–4]. For example, IoT is optimized with 5G network to expand spectrum resources and supply large data volume business [5], simultaneous wireless information and power transfer has been proposed for energy efficiency and ubiquitous links [6]. With the development of IoT, Internet of Vehicles (IoV) is evolving as a new theme of research from traditional vehicular Ad hoc networks (VANETs) [7, 8] to enable more intelligent driving experiences such like vehicle localization, behavior analysis even automatic driving [9–11]. For these applications, the vehicle speed estimated by perception operation is an essential input. The accurate speed estimation makes the cognitive computing based on it reliable in complex traffic environment, thus providing further support for intelligent decision-making [12, 13].

One way to obtain vehicle speed is through Doppler shift estimation in mobile communication and subsequent conversion calculation [14]. Several estimators had been proposed, but most of them suffered from additive white Gaussian noise (AWGN) [15–18]. Although maximum likelihood methods [19, 20] took account of the noise effects for accuracy enhancement, an exhausted search was required, making them

not competitive for real-time applications. On the other hand, to adapt the communication receiver to wireless propagation, signal-to-noise ratio (SNR) estimation is also needed [21]. To reduce realization cost, Doppler shift and SNR were jointly estimated [22–24]. A nonparametric estimator based on peak search in frequency domain was proposed, but its Doppler shift estimation was not reliable [22]. For improvement, signal processing methods including double sampling rate (DSR), autocorrelation function (ACF) and level crossing rate (LCR) had been applied in estimator, making the estimator also applicable in noisy scenarios [23, 24].

In former research on ACF-DSR estimator [23], though the simulation results showed a good performance in a wide range of velocities and SNRs, the analysis should be further refined. Because the fixed integer ratio of two sampling intervals limits estimator performance, and the perfect estimation of original Doppler shift does not work in practice. Therefore, an improved Doppler shift estimator taking account of nonideal deviation is established in this paper, and factional ratio is also applied to analyze its effect on estimator performance under the assumption of large estimation error. By Monte Carlo simulations, two better ratio of sampling intervals are obtained, in which the fractional one can also benefit computation reduction. Simultaneously, it is demonstrated that the optimized ACF-DSR estimator with better sampling interval setting can produce better Doppler shift and SNR estimation. In contrast to previous methods, the optimized ACF-DSR estimator performs best, which consequently produces the most accurate speed estimates.

The paper is organized as follows: the original ACF-DSR estimator is introduced in Sect. 2. Then, in Sect. 3, the optimized estimator is formulated, and the analysis of sampling intervals is achieved. Finally, in Sect. 4, the superiority of the optimized estimator is demonstrated by numerical results. Conclusion is given in Sect. 5.

2 ACF-DSR estimator

In this paper, it is assumed that a band-limited pilot signal is transmitted over a Rayleigh fading channel. The ACF calculation for Rayleigh fading channel can be expressed as:

$$R(k) = \sigma_l^2 J_0(2\pi f_d k T_s) \tag{1}$$

where σ_l^2 and f_d represent the actual channel variance and Doppler shift, T_s is the pilot symbol interval, $J_0(\cdot)$ denotes the first kind Bessel function [23].

To estimate Doppler shift and SNR jointly, the channel ACF is firstly estimated base on channel estimates, i.e.,

$$\hat{R}(k) = \frac{1}{K-1} \sum_{i=0}^{K-1} \hat{c}_l(i) \hat{c}_l^*(i+k) \tag{2}$$

where $\hat{c}_l(i)$ is the channel estimates (i is the discrete time index and l denotes the path index), and k is the index for discrete time delay. Besides, K is the total sample number which should be larger enough to ensure the time length larger than the fading period. Then, the original Doppler shift estimator based on ACF can be given by

$$\hat{f}_d = \frac{\sqrt{2\left(1-\sqrt{\hat{R}(1)\big/\hat{R}(0)}\right)}}{\pi T_s} \tag{3}$$

Above estimator is known bias when AWGN exists. For improvement, the ACF was adapted for noisy scenarios by setting $R(0) = \sigma_l^2 + \sigma_z^2$, and its estimation $\hat{R}(0)$ was correspondingly modified [23].

Above Doppler shift estimation is original, to enhance accuracy also to obtain the SNR and Doppler shift estimations jointly, the DSR technique was applied [23]. It is realized by establishing equation after getting an original Doppler shift estimation, i.e.,

$$\hat{f}_d = f_d \cdot \sqrt{\frac{1-\sqrt{\frac{\gamma_s}{\gamma_s+1}J_0(2\pi f_d T_s)}}{1-\sqrt{J_0(2\pi f_d T_s)}}} \tag{4}$$

where $\gamma_s = \sigma_l^2/\sigma_z^2$ denotes the SNR.

In above equation, there are two unknown parameters, i.e., Doppler shift f_d and SNR γ_s. For joint estimation through equations solving, two sampling intervals $T_{s1} = mT_s$ and $T_{s2} = nT_s$ (m, n are integers and $m < n$) are adopted, then two equations based on two original Doppler shift estimations ($\hat{f}_{d1}$ and $\hat{f}_{d2}$) are formulated as below, in which the fourth order approximation of Bessel function is adopted to enables Doppler shift estimator practicable in high-speed scenarios.

$$\hat{f}_{d1} = \frac{\sqrt{2-\sqrt{\frac{\gamma_s}{\gamma_s+1}}\left(2-(m\pi f_d T_s)^2\right)}}{m\pi T_s} \tag{5}$$

$$\hat{f}_{d2} = \frac{\sqrt{2-\sqrt{\frac{\gamma_s}{\gamma_s+1}}\left(2-(n\pi f_d T_s)^2\right)}}{n\pi T_s} \tag{6}$$

Solving above equations, the following joint estimation is obtained.

$$\hat{f}_d = \frac{1}{\pi}\sqrt{\frac{2(A-1)}{An^2T_s^2 - m^2T_s^2}} \quad \hat{\gamma}_s = \frac{1}{B^2-1} \tag{7}$$

where $A = \frac{2-(m\pi\hat{f}_{d1}T_s)^2}{2-(n\pi\hat{f}_{d2}T_s)^2}$ and $B = \frac{(\hat{f}_d n)^2-(\hat{f}_d m)^2}{(\hat{f}_{d2} n)^2-(\hat{f}_{d1} m)^2}$.

For above two sampling intervals $T_{s1} = mT_s$ and $T_{s2} = nT_s$, the increase in $m(n)$ results the decrease in channel sampling rate, thus the computation cost can be definitely reduced when doing ACF calculation. At the same time, the sampling theory must be held, i.e., the sampling rate must be larger than two times of the channel bandwidth. Correspondingly, the following inequation should be satisfied, which limits the value choice of (m, n).

$$f_m < \frac{0.5}{\max(m,n)} \left(f_m = f_d T_s\right) \tag{8}$$

Thus, for the application of ACF-DSR estimator, the maximum value of the normalized Doppler shift f_m should be firstly estimated to determine the integer values for (m, n). It is explicit that the smaller value of f_m enlarges the value range for (m, n).

3 Analysis and optimization of ACF-DSR estimator

3.1 Algorithm model establishment

Because of nonideal channel model or sample number for estimation, the original Doppler estimation makes Eqs. (5) and (6) untenable. To enhance the authenticity and reliability of the analysis in this section, an estimation deviation Δ is considered existing between the values on both sides of the equal sign in (5) and (6). According to our simulations, the following remarks have been concluded.

- When the actual Doppler shift f_d and SNR γ_s are increasing, the estimation deviation Δ is generally decreasing. Besides, the maximum of the observed Δ in simulation can nearly be 23% of f_d.
- The larger sampling interval leads to smaller deviation, i.e., $T_{s1} < T_{s2} \Rightarrow \Delta_1 > \Delta_2$. Because the noise bandwidth becomes smaller when larger sampling interval is applied, thus SNR is equivalently increased, which results in smaller deviation.
- The deviation $\Delta_1(\Delta_2)$ is approximately a linear decreasing function of $m(n)$.

Based on above remarks, Eqs. (5) and (6) for joint Doppler shift and SNR estimations in (7) are reformulated as

$$\hat{f}_{d1} = \frac{\sqrt{2 - \sqrt{\frac{\gamma_s}{\gamma_s+1}}\left(2 - (m\pi f_d T_s)^2\right)}}{m\pi T_s} + \frac{\Delta}{m} \tag{9}$$

$$\hat{f}_{d2} = \frac{\sqrt{2 - \sqrt{\frac{\gamma_s}{\gamma_s+1}}\left(2 - (n\pi f_d T_s)^2\right)}}{n\pi T_s} + \frac{\Delta}{n} \tag{10}$$

3.2 Choice of sampling intervals

In this part, above two Eqs. (9) and (10) are utilized to analyze the effect of two sampling intervals, i.e., the values of (m, n). In this paper, the maximum value of the normalized Doppler shift f_m is prespecified 0.1 for simulation and analysis. Due to the limit in (8) and the assumption as $m < n$, the maximum value for n is 5. Thereby, there are two types of value choice for (m, n):

- n/m is integer: $m = 1$, and $n \in \{2, 3, 4, 5\}$.
- n/m is fraction: m and n are relatively prime and $2 \leq m < n \leq 5$.

In this paper, the estimation deviation Δ is pre-specified when doing simulation for analysis. For reliability, it is relaxed to 30% from the observed maximum 23%. The analysis for different n/m is conducted by two cases according to whether ΔT_s is fixed or

changing. In addition, the mean square error (MSE) of the final Doppler shift estimation $\hat{f}_d$ is applied for comparison, which is defined by

$$E_f = E\left[\left|\hat{f}_d / f_d - 1\right|^2\right] \tag{11}$$

where $E[\cdot]$ denotes the expectation operation.

3.2.1 Case I (ΔT_s is fixed)

In this case, $f_m \in \{0.01 : 0.01 : 0.1\}$, $SNR \in \{0 : 3 : 30\}$ and ΔT_s is fixed 0.03, which corresponds to the worst case (estimation deviation reaches 30% of f_d). After computer simulation, the MSE of Doppler shift estimation is shown in Fig. 1, in which different values of m and n make the resulted MSE fluctuates. From Fig. 1a, it can be found that larger n can result in smaller MSE. When using the same n, the fraction n/m outperforms integer n/m, and larger m is better for fraction n/m. Obviously, the originally used $n/m = 2$ in [23] is the worst choice.

In Fig. 1b, the SNR increasing makes the MSE changing like a concave curve. Relatively, the turning point that the MSE changes from decreasing to increasing is latter for lager n. Though in previous remarks, larger f_d and γ_s leading to smaller deviation Δ is derived, the final estimation $\hat{f}_d$ obtained by equations solving is nonlinearly and comprehensively affected by f_d, γ_s and Δ. When negative effects outweigh positive effects, the MSE curve rises. Therefore, in Fig. 2, we can also find concave curves of MSE changing for different f_m ($f_d = f_m / T_s$), in which the negative effects is more evident when f_m is smaller.

3.2.2 Case II (ΔT_s is changing)

In this case, ΔT_s is changing from 0.005 to 0.03 by step 0.005. Figure 3 displays the MSE of Doppler shift estimation for different ΔT_s, which increases as ΔT_s becomes larger. For small ΔT_s, the increase in MSE is rapid and the performances of n/m's are not consistent with previous performance presented in Fig. 1. Such deviation suggests us to choose the best sampling intervals (namely m and n) carefully. For further analysis, the MSEs are averaged over ΔT_s's, results are shown in Fig. 4, and nearly the same conclusion found in Figs. 1 and

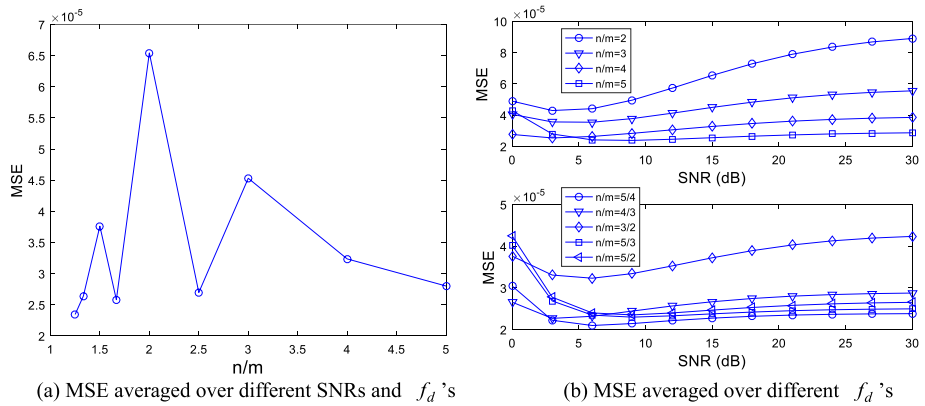

(a) MSE averaged over different SNRs and f_d's (b) MSE averaged over different f_d's

Fig. 1 The MSE of Doppler shift estimation

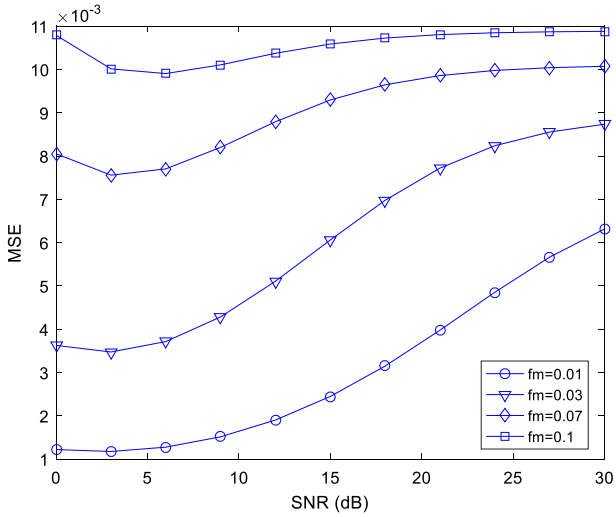

Fig. 2 The MSE of Doppler shift estimation: n/m = 2

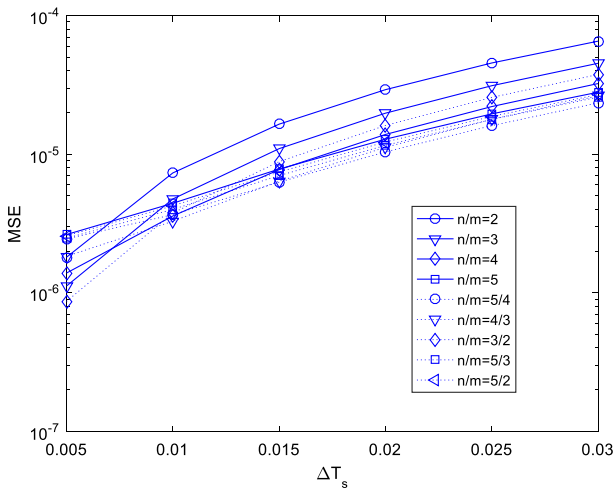

Fig. 3 The MSE of Doppler shift estimation for different ΔT_s's

2 can be obtained. Hence, the following analysis is carried out with the same parameter setting as that in Case I.

According to all above presentations and analysis, it seems that $n/m = 5/4$ is the best choice, but it is hard to confirm because the deviation is modeled approximately, and the estimator can be sensitive for two very close sampling intervals. To find a better n/m for practical use, another performance called mismatch MSE (mMSE) is applied.

$$E_f(n,m) = \frac{1}{M-1} \sum_{1 \le m_t < n_t \le 5} (\hat{f}_d(n,m) - \hat{f}_d(n_t,m_t))^2 \tag{12}$$

where M is the total number of (n,m). Actually, $E_f(n,m)$ can be viewed as a measurement for estimation stability under the principle of Least-Square (LS). The most stable n/m, i.e., the one results in smallest $E_f(n,m)$, can also be robust against nonideal factors.

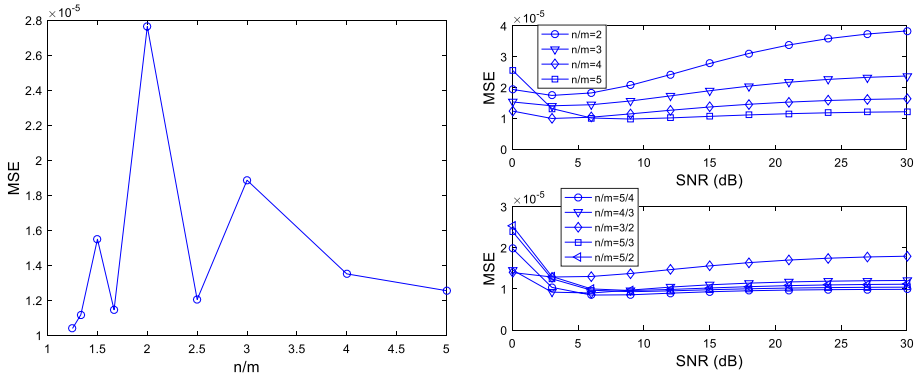

(a) MSE averaged over different SNRs, f_d's and ΔT_s's and ΔT_s's

(b) MSE averaged over different f_d's

Fig. 4 The MSE of Doppler shift estimation for different ΔT_s's

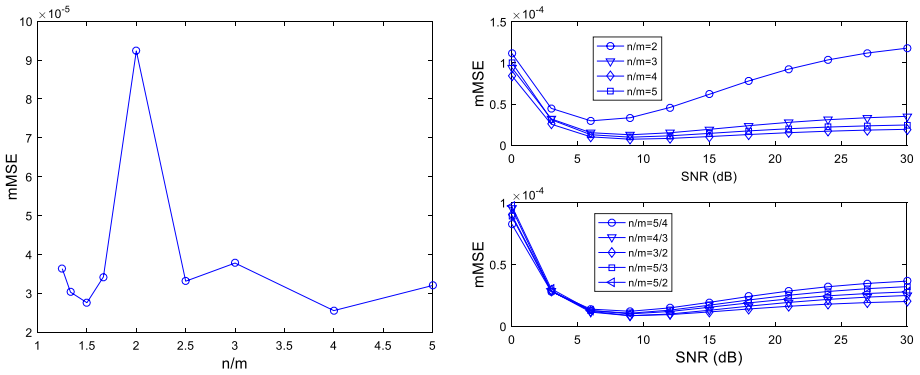

(a) mMSE averaged over different SNRs and f_d's

(b) mMSE averaged over different f_d's

Fig. 5 The mismatched MSE (mMSE) for Doppler shift estimates

The mMSE results are presented in Fig. 5. It is obvious that $n/m = 2$ is the worst choice. Moreover, a larger gap between n and m or a smaller n for fraction n/m can lead to higher stability of mMSE. Based on all figures and above comprehensive analysis, $n/m = 4/3$ and $n/m = 4$ are two better choices for the scenario in this paper. On the other side, the fraction $n/m = 4/3$ has an advantage of computation reduction over $n/m = 4$ for its larger m.

4 Simulation

In this section, the optimized ACF-DSR method with better choices of n/m ($n/m = 4$ and $n/m = 4/3$) is further demonstrated in comparison with previous methods including the phase difference method [15], the original ACF-DSR method ($n/m = 2$) [23], the ACF method [16], the LCR-DSR method with fitting [24] and the improved LCR-DSR (without fitting) [25]. Computer simulations are executed for estimator comparison, in which the Jakes channel model is adopted. Besides, the pilot symbol interval T_s is 0.2 ms, the carrier frequency is 2.11 GHz. The vehicle speed range is 30–240 km/h and its corresponding Doppler shift is 58.6–468.8 Hz [24].

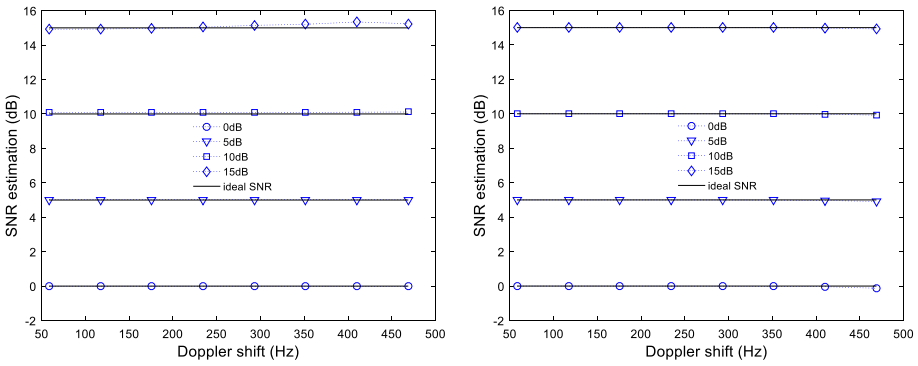

Fig. 6 The SNR estimation performance of the optimized ACF-DSR estimator

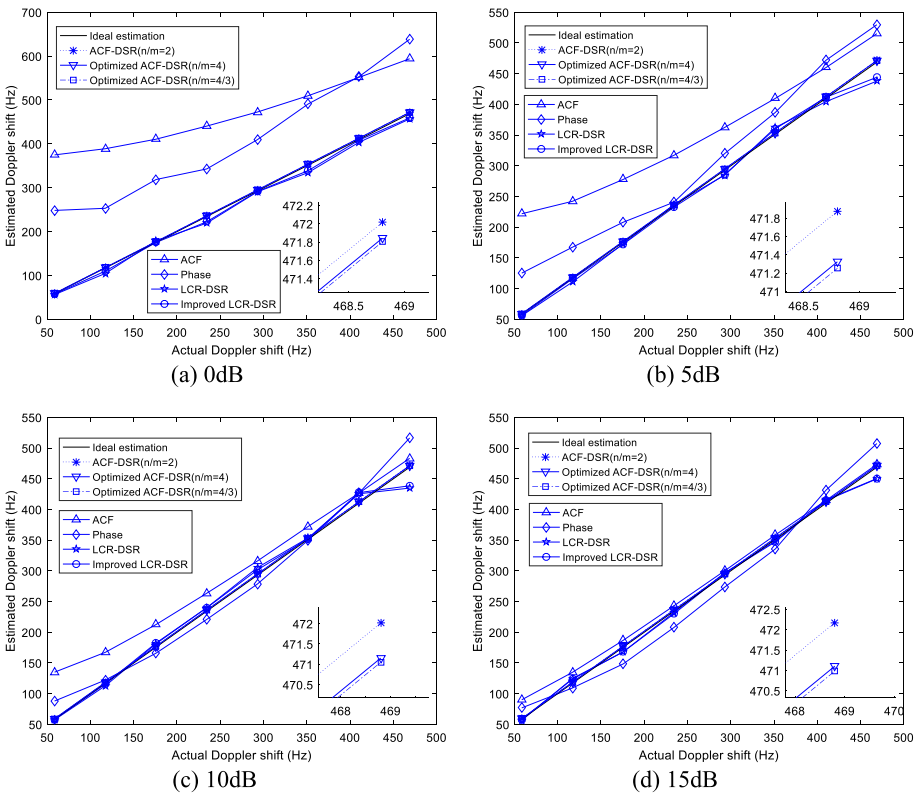

Fig. 7 The Doppler shift estimation comparison of the optimized ACF-DSR method and previous methods

The simulated results of SNR estimation are presented in Fig. 6. From this figure, it is explicit that SNR can be very precisely estimated by the optimized ACF-DSR estimator. Relatively, the estimations in low SNR scenarios are more accurate than those in high SNR scenarios. For reliable vehicle speed estimation in IoV, the Doppler shift estimation performance is more concerned. Figure 7 shows the comparison of Doppler shift estimations by different methods. Among, the phase difference method and the ACF method performs badly, because they cannot eliminate the influence of AWGN. On the other

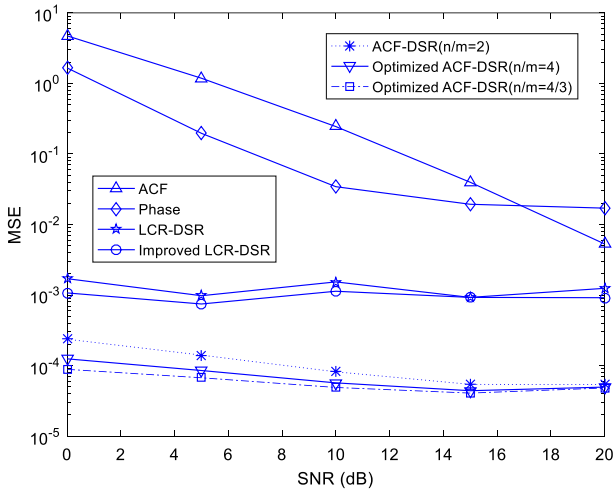

Fig. 8 The MSE comparison of the optimized ACF-DSR method and previous methods

Table 1 The comparison of vehicle speed estimation

SNR	0 dB			10 dB		
Actual speed (km/h)	**60**	**150**	**240**	**60**	**150**	**240**
Phase	129.6005	209.7732	326.8913	67.5705	142.6716	264.4130
ACF	169.1074	241.9821	304.1149	85.6709	161.8714	247.4229
LCR-DSR	53.5621	148.9060	233.8882	57.7539	156.3410	222.6136
Improved LCR-DSR	56.2855	149.3620	235.0838	59.2265	154.4677	224.5373
ACF-DSR ($n/m=2$)	61.5759	152.1843	243.0255	61.3410	151.7453	242.3683
ACF-DSR ($n/m=4$)	60.4510	151.0596	241.5793	60.5737	150.9849	241.2269
ACF-DSR ($n/m=4/3$)	60.4480	151.0356	241.5589	60.5352	150.8749	241.1746

hand, the three ACF-DSR methods perform approximately, and all of them are slightly better than the LCR-DSR method and its improved version. Among these two LCR-DSR methods, fitting operation is not applied in the LCR-DSR, thus its advantage over the LCR-DSR method with fitting is limited. Moreover, the figures are partially enlarged for detail comparison, from which we can see that the optimized ACF-DSR method yields the best performance.

Figure 8 compares different estimators by averaged MSE of Doppler shift estimation along SNR dimension. Due to that the improved algorithm modeling takes account of estimation deviation, the optimized ACF-DSR method is robust to AWGN, thus it can outperform the phase difference method, two LCR-DSR methods and the ACF method. Among the ACF-DSR methods (the optimized and the original) using different n/m, the optimized with $n/m = 4$ or $n/m = 4/3$ performs better than the original with $n/m = 2$, and the optimized with $n/m = 4/3$ is slightly better than the other with $n/m = 4$. Moreover, the optimized with $n/m = 4/3$ also has an advantage on computation, which can be reduced to nearly one third of the other with $n/m = 4$.

According to the Doppler shift estimates, the vehicle speed estimation can be obtained by linear transformation. The comparison of vehicle speed estimation for two SNRs ({0, 10} dB) and three actual speeds ({60, 150, 240} km/h) is shown in Table 1. As can be

seen from the table, the phase difference method and the ACF method are obviously the two worst estimators. Moreover, the improved LCR-DSR is slightly better than the LCR-DSR, but both are worse than the ACF-DSR methods. Among the ACF-DSR methods, the optimized ($n/m = 4$ and $n/m = 4/3$) perform better than the original with $n/m = 2$ for their improved speed estimations. Thus, the optimized ACF-DSR estimator can utilized to serve speed-related applications in IoV.

5 Conclusion

In this paper, the ACF-DSR estimator for joint Doppler shift and SNR is optimized by taking estimation deviation into algorithm model and selecting better sampling intervals. Its effectiveness and reliability are confirmed by simulations. Moreover, the estimator is simple to realize in mobile communication with either code-multiplexed or time-multiplexed pilot signals, and its accurate Doppler shift estimation can be utilized for vehicle speed estimation in IoV.

Abbreviations

ACF: Autocorrelation function; DSR: Double sampling rate; IoT: Internet of things; IoV: Internet of Vehicles; VANETs: Vehicular Ad hoc networks; AWGN: Additive white Gaussian noise; SNR: Signal-to-noise ratio; LSR: Level crossing rate; WSSUS: Wide-sense stationary and mutually uncorrelated scattering; MSE: Mean square error; mMSE: Mismatch mean square error; LE: Logarithmic envelope.

Acknowledgments

The authors would like to thank Zhejiang Gongshang University, Zhejiang Provincial Key Laboratory of New Network Standards and Technologies for their support and anyone who supported the publication of this paper.

Author contributions

JYH contributed to the development of ideas. JGW and LY conducted algorithm modeling, numerical analysis, and wrote the paper. XFF also contributed paper writing. ZWN and ZJX proofread and revised this paper. All authors read and approved the final manuscript.

Funding

This paper was sponsored by the Natural Science Foundation of Zhejiang Province (Grant No. LQ21F010008), and Zhejiang Gongshang University, Zhejiang Provincial Key Laboratory of New Network Standards and Technologies (Grant No. 2013E10012).

Availability of data and materials

Data sharing is not applicable to this article.

Declarations

Competing interests

The authors declare that they have no competing interests.

Author details

[1]School of Information and Electronic Engineering, Zhejiang Gongshang University, Hangzhou 310018, China. [2]School of Management and E-Business, Zhejiang Gongshang University, Hangzhou 310018, China. [3]Zhejiang Provincial Key Laboratory of Information Processing, Communication and Networking, Hangzhou 310012, China.

Received: 23 January 2022 Accepted: 2 April 2022
Published online: 15 April 2022

References

1. X. Liu, X. Zhang, NOMA-based resource allocation for cluster-based cognitive industrial Internet of Things. IEEE Trans. Ind. Inform. **16**(8), 5379–5388 (2019)
2. X. Liu, X.B. Zhai, W. Lu, C. Wu, QoS-guarantee resource allocation for multibeam satellite industrial Internet of Things with NOMA. IEEE Trans. Ind. Inform. **17**(3), 2052–2061 (2019)
3. H.N. Dai, Z. Zheng, Y. Zhang, Blockchain for Internet of Things: a survey. IEEE Internet Things J. **6**(5), 8076–8094 (2019)
4. S. Li, L. Da Xu, S. Zhao, 5G Internet of Things: a survey. J. Ind. Inf. Integr. **10**, 1–9 (2018)
5. X. Liu, X. Zhang, Rate and energy efficiency improvements for 5G-based IoT with simultaneous transfer. IEEE Internet Things J. **6**(4), 5971–5980 (2019)

6. X. Liu, X. Zhang, M. Jia et al., 5G-based green broadband communication system design with simultaneous wireless information and power transfer. Phys. Commun. **28**, 130–137 (2018)
7. J. Zhao, Q. Li, Y. Gong, K. Zhang, Computation offloading and resource allocation for cloud assisted mobile edge computing in vehicular networks. IEEE Trans. Vech. Technol. **68**(8), 7944–7956 (2019)
8. F. Li, K.Y. Lam, Z. Ni, D. Niyato, X. Liu, L. Wang, Cognitive carrier resource optimization for internet-of-vehicles in 5G-enhanced smart cities. IEEE Netw. (2021). https://doi.org/10.1109/MNET.211.2100340
9. J. Yu, H. Zhu, H. Han, Y.J. Chen et al., Senspeed: sensing driving conditions to estimate vehicle speed in urban environments. IEEE Trans. Mob. Comput. **15**(1), 202–216 (2015)
10. J. Zhao, X. Sun, Q. Li, X. Ma, Edge caching and computation management for real-time Internet of Vehicles: an online and distributed approach. IEEE Trans. Intell. Transp. Syst. **22**(4), 2183–2197 (2021)
11. J. Hua, Y. Yin, A. Wang, Y. Zhang, W. Lu, Geometry-based nonline-of-sight error mitigation and localization in wireless communications. Sci. China Inf. Sci. **62**(10), 1–15 (2019)
12. M. Pirani, E. Hashemi, A. Khajepour, B. Fidan et al., Cooperative vehicle speed fault diagnosis and correction. IEEE Trans. Intell. Transp. Syst. **20**(2), 783–789 (2018)
13. J. Zhao, P. Dong, X. Ma, X. Sun, D. Zou, Mobile-aware and relay-assisted partial offloading scheme based on parked vehicles in B5G vehicular networks. Phys. Commun. **42**, 101163 (2020)
14. J.Y. Hua, D.H. Yuan, G. Li, L.M. Meng, Accurate estimation of Doppler shift in mobile communications with high vehicle speed. Int. J. Commun. Syst. **27**(12), 3515–3525 (2014)
15. J. Hua, B. Sheng, X. You, The phase probability distribution of general clarke model and its application in Doppler shift estimation. IEEE Antennas Wirel. Propag. Lett. **4**, 373–377 (2005)
16. C. Xia, K.D. Mann, J.C. Olivier, Mobile speed estimation for TDMA based hierarchical cellular systems. IEEE Trans. Vech. Technol. **50**(4), 981–991 (2001)
17. A. Sampath, J.M. Holtzman, Estimation of maximum Doppler frequency for handoff decisions, in *The 43rd Vehicular Technology Conference* (1993), pp. 859–862
18. W. Sheng, S.D. Blostein, SNR-independent velocity estimation for mobile cellular communication systems, in *IEEE ICASSP'02*, vol 3 (2002), pp. 2460–2472
19. A. Dogandzic, B. Zhang, Estimating Jakes' Doppler power spectrum parameters using the whittle approximation. IEEE Trans. Signal Process. **53**(3), 987–1005 (2005)
20. L. Krasny, H. Arslan, D. Koilpillai, S. Chennakeshu, Doppler spread estimation in mobile radio systems. IEEE Commun. Lett. **5**(5), 197–199 (2001)
21. N.C. Beaulieu, A.S. Toms, D.R. Pauluzzi, Comparison of four SNR estimators for QPSK modulations. IEEE Commun. Lett. **4**(1), 43–45 (2000)
22. J. Hua, L. Meng, X. Xu, D. Wang, X. You, Novel scheme for joint estimation of SNR, Doppler, and carrier frequency offset in double-selective wireless channels. IEEE Trans. Vech. Technol. **58**(3), 1204–1217 (2009)
23. J. Hua, L. Meng, Z. Xu, D. Wang, A new method for SNR and Doppler shift estimation in wireless propagations. J. Electromagn. Waves Appl. **21**(15), 2431–2441 (2007)
24. J. Hua, L. Meng, G. Li, D. Wang, B. Sheng, X. You, Joint estimation of channel parameters for very low signal-to-noise ratio environment in mobile radio propagations. Radio Sci. **45**(4), 1–8 (2010)
25. S.Y. Jiang, J.Y. Hua, W.D. Lu et al., Evaluation and improvement of LCR-DSR channel parameter estimator in mobile communications. Sci. Sin. Inform. **48**, 349–358 (2018). (**in Chinese**)

Publisher's Note